Australian Journal of Basic and Applied Sciences, 5(5): 955-966, 2011
ISSN 1991-8178

A Numercial Comparison of Single-phase Forced Convective Heat Transfer Between Round Tube and Round Microchannel Heat Exchangers

[1]P. Mohajeri Khameneh, I. Mirzaie, N. Pourmahmoud, S. Majidyfar, [2]S.H. Azizi

[1]Department of Mechanical Engineering, Faculty of Engineering, Urmia University, Urmia, 57169-33111, Iran.
[2]Department of Mechanical Engineering, Bandar Lenge Branch, Islamic Azad University, Bandar Lengeh, 79715-363, Iran.

Abstract: Three dimensional simulations of the single-phase laminar flow and forced convective heat transfer of water in round tube and round microchannel heat exchangers were investigated numerically. This numerical method was developed to measure heat transfer parameters of round tube and round microchannel tube geometries. Then, similarities and differences were compared between different geometries. The geometries and operating conditions of those indicated heat exchangers were created using a finite volume-based computational fluid dynamics technique. In this article, at each Z-location variation of dimensionless local temperature, non-dimensional local heat flux variation and dimensionless local Nusselt number distribution along the tube length were compared between round tube and round microchannel heat exchangers. Consequently, averaged computational Nusselt number was obtained for those indicated models and then validation study was performed for round tube counter flow type heat exchanger model. Finally, all of these numerical results for both kind of geometries in counter flow heat exchangers were discussed in details.

Key words: Heat exchanger; Numerical simulation; Laminar flow; Round tube; Round Microchannel.

INTRODUCTION

Improvements in technology substituting itself with smaller, thinner, carryable and quicker devices. From the other point of view, these technological developments also demand more compact thermal solutions. Hence, air conditioning industry has been attempting to acquire higher productivity level and greater supplies dependability. When the purpose becomes concurrently decrease equipments extent and reduce the cost, manufacturers will have problems and troubles to satisfy the energy efficiency necessities (Keogh, 2007). After the earliest investigation of heat transfer in microstructures by Tuckermann and Pease (1981), microchannel heat exchangers became an inventive and improving method in thermal applications. Having an enormous efficiency likened with its smaller and thinner geometry made microchannel heat exchangers a significant feasible solution in different industries. Compared to current round tube heat exchangers, the efficiency and the rate of heat transfer in microchannel heat exchangers has a higher value. This increase in heat exchanger effectiveness permits the microchannel heat exchanger to be to be smaller and yet have the same performance as a conventional round tube heat exchanger. Microchannel technology is very usual for automotive air conditioning implementations because of its small size, which indicates the technology has conquered the critical manufacturing difficulties.

In early 1980, experimental investigation of the fluid flow and heat transfer characteristics in microchannel was started. Tuckermann *et al.*'s (1981; 1982) investigations motivated a lot of researchers to recognize fluid flow and its influences on convective heat transfer coefficient in microchannels. After this initial study other probes have supported the earliest results and have served to demonstrate remarkably high levels of heat elimination that can be performed using microchannel structures. In 1995, a collective study between Peng and Peterson (1995) was aimed to investigate the rectangular microchannel port size effect on thermal properties

Corresponding Author: P. Mohajeri Khameneh, Department of Mechanical Engineering, Faculty of Engineering, Urmia University, Urmia, 57169-33111, Iran,
Tel/Fax: +98-21-88977985 Mob: +98-912-5263123
E-mail: pedram.mohajeri@gmail.com

of the fluid. It was obtained that because of the excessive size decrease in the channel port an unexpected change can take place in thermophysical characteristics which increases the Reynolds number of the fluid flow. Consequently, a transition from laminar to turbulent region can be occurred at lower Reynolds number than customary and usual size channels. In 2000, convective heat transfer in parallel models (I-tube) and series model (U-tube) was studied experimentally by Rahman (2000). Water was used as working fluid to explore the changes of the Nusselt number and pressure drop. It was deduced that at any given Reynolds number, the higher Nusselt number was observed at the entrance region in comparison with outlet region due to the beginning of boundary layer formation.

In the early 21st century a numerical study of three-dimensional conjugate heat transfer in microchannel heat sinks was demonstrated by Federov and Viskanta (2000). Navier-Stokes equations was employed as governing equations to analyze incompressible laminar flow. In addition, it was shown that Navier-Stokes equations are able to supply precise numerical simulations and answers for laminar flow and conjugate heat transfer investigations in microchannels. Also, another numerical study in the field of conjugate heat transfer in microchannel heat sinks was presented by Ambatipudi and Rahman (2000). First, highest local Nusselt number was reported at the entrance due to the development of thermal boundary layer. In addition, it was mentioned that with a higher channel depth and lesser solid available between the heater and the coolant, smoother temperature distribution will be obtained. Furthermore, it was concluded that outlet temperature and also the maximum temperature inside the solid channel can be decreased with an increase in Reynolds number because in this case a larger mass flow rate is available to remove the heat.

Another numerical study between Qu and Mudavar (2002) was explored three dimensional fluid flow in rectangular microchannel heat sinks. Their study was aimed to appraise local and average thermal properties such as temperature, heat flux and Nusselt number in microchannels. In addition, it was concluded that the maximum value for Nusselt number and heat flux was occurred at the channel inlet and on the other hand, the Nusselt number and heat flux value near the channel corners was approached to zero. Furthermore, it was stated that the increase of the Reynolds number which raises the fully developed region length led to the enhancement in heat transfer.

The differences between the classical correlations and the experimental results were indicating in early investigations. However, some recent investigations have asserted that conventional size correlations were in a good agreement with experimental results in microchannel heat exchangers. In this connection, the heat transfer of laminar distilled water flow in microtubes was explored by Lelea and coworkers (Lelea, 2004). The experimental results were approved that conventional and classical theories are applicable for water flow within 0.1, 0.2, 0.5 mm diameter microchannels. Furthermore, it was concluded that if the total length of the tube is heated, the multiplication value of friction factor and the Reynolds number can be equal to the conventional constant, $f.Re = 64$. However, lower $f.Re$ values were appraised if the partial heating is occurred.

In 2009, deviations between classical correlations and experimentally microchannel results have been studied Mokrani *et al.,* (2009). It was deduced that after decreasing the measurement errors and clarifying the entrance zone effect, conventional size correlations can be applied to identify heat transfer analysis in microchannels. In addition, transition from laminar to turbulent region in microchannels was occurred in a similar range of Reynolds number that it was observed in conventional size channels. Recently, Wang *et al.,* (2009) have presented numerical and experimental investigation of forced convective heat transfer in a microchannel having a hydraulic diameter of 155mm with negligible axial heat conduction. Then, numerical simulations were compared with experimental results and it was found that numerical predictions were in a good agreement with experimental results. This compatibility between numerical and experimental results confirm that classical Navier-Stokes and energy equations are capable for modelling of forced convection in microchannel heat exchangers having a hydraulic diameter as small as 155 μm.

The present work was undertaken to compare heat transfer properties of round tube and round microchannel (RMC) tube geometries numerically. In this article, the refrigerant side heat transfer coefficient was investigated for those indicated heat exchangers. Then, similarities and differences between those geometries were discussed precisely. As a test environment, identical single phase, laminar, counter flow water jacket was simulated around two kind of tubes. Finally, according to the changes within the surrounding water jacket flow, averaged and local heat transfer characteristics were compared and discussed for round tube and round microchannel counter flow type heat exchangers.

2. Description of Numerical Simulation Procedure:

In this article, a numerical method is developed to calculate heat transfer parameters of round tube and round microchannel heat exchanger geometries and then thermal properties for those indicated heat exchangers are compared and discussed precisely. The aim of this study is to investigate the refrigerant side heat transfer characteristics by simulating round tube and round microchannel counter flow type heat exchangers. In this numerical method, three dimensional computational domain is used for simulating internal cooling capacity for each heat exchanger.

In order to analyze the maximum heat transfer capacity of heat exchanger tubes, counter flow type heat exchanger is selected to provide higher temperature difference between hot and cold fluids. As a reference study, Padhmanabhan's (2008) investigation is selected to create round tube and round microchannel tube geometries in this simulation. In order to have a reasonable comparison, identical conditions is required for surrounding water jacket around both kind of heat exchanger tubes. Additionally, to identify local and averaged thermal properties, obtained results are compared and then those numerical results for round tube and round microchannel counter flow heat exchangers are discussed in details.

3. Assumptions of Physical Models:

In this investigation, tube geometries and boundary conditions for round tube and round microchannel heat exchangers are defined based on Padhmanabhan et al., (2008) study. As a considerable assumption in those indicated models, aluminium with 30 mm diameter is defined for water jacket tube. Whereas, the hydrodynamic entrance region (L_h) is shorter than the tube length (L_{tube}), fully developed and laminar water flow is assumed in this simulation. Which, L_h is calculated based on Langhaar *et al.*, s correlation given in Incropera *et al.*, s (1996) text book. Based on Eq. (1), L_h value is obtained according to Re_{Dh} and D_h which is shown as:

$$L_h \cong 0.05 Re_{D_h} D_h \quad (1)$$

In addition, further assumptions which are exerted in this simulation, are presented below:

- The governing equations based on Navier-Stokes equations can be used to describe the physical models.
- The process is steady and the fluid is incompressible.
- The body forces are neglected.
- The thermal properties of water are varying with temperature and the thermal properties of solid are constants.
- "No slip boundary condition" is selected at all solid boundaries.
- Radiation heat transfer and natural convective heat transfer are neglected.

4. Computational Pre-processing and Boundary Conditions:

4.1. Round Tube Heat Exchanger Computational Pre-processing:

As it mentioned earlier, round tube counter flow heat exchanger is simulated in this numerical method. Water jacket is cooled along the tube length (L_{tube}) and local thermal properties are evaluated in laminar region. Round tube counter flow heat exchanger configuration which is simulated in this numerical method, is presented in Fig. 1 and also, a cross section of this round tube heat exchanger is shown in Fig. 2.

In order to increase the computational efficiency and by using "SYMMETRY" boundary conditions, quarter geometry is created according to heat exchanger tube's geometric specifications which are listed in table 1.

This round tube heat exchanger dimensions are expressed with round tube's inner radius ($R_{round\text{-}tube\ in}$), round tube thickness ($t_{round\text{-}tube}$), round tube outer length ($L_{round\text{-}tube}$), jacket radius (R_{jacket}) and overall tube length (L_{tube}).

Table 1: Geometric parameters for round tube heat exchanger.

Parameter	Length (mm)
$R_{round\ tube\ in}$	4.84
$t_{round\ tube}$	0.3
R_{jacket}	15
$L_{round\ tube}$	8.08
L_{tube}	1200

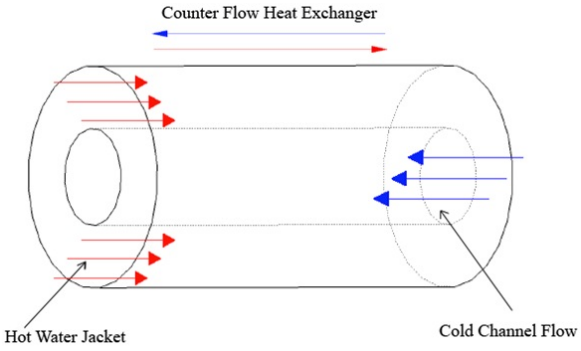

Fig. 1: Sketch of the round tube counter flow type heat exchanger.

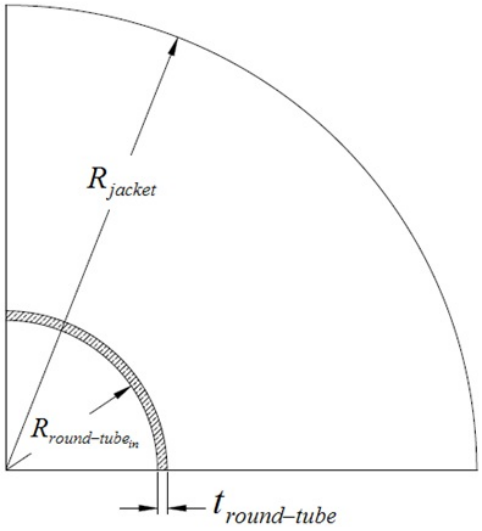

Fig. 2: Cross-section of round tube heat exchanger.

Furthermore, equally spaced grid points are applied based on round tube's inner radius ($R_{round\text{-}tube\ in}$) and jacket radius ($R_{jacket}$) to round tube thickness ($t_{round\text{-}tube}$) ratio, respectively. For the arc length, round tube outer length ($L_{round\text{-}tube}$) to channel thickness ratio is applied to create equal tangential grid spacing. Resultant mesh quality for this grid study is presented in Fig. 3. Finally, it should be noted that this grid system is adopted after a grid independence examination.

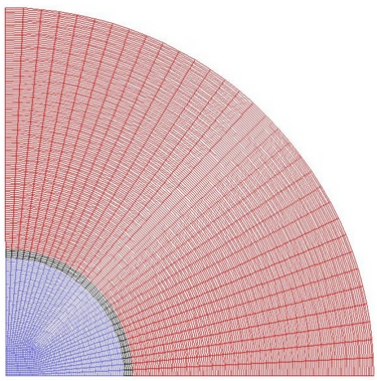

Fig. 3: Partial geometry and grid generated of round tube heat exchanger.

4.2. Round Microchannel Heat Exchanger Pre-processing:

After an extensive investigation on previous studies, it is concluded that a transition from laminar to turbulent region is occurred at lower Reynolds number in microchannels due to sudden changes in fluid thermophysical properties. Therefore, a smaller grid distance both on port faces and through flow direction is exerted to have a precise response of fluid flow in microchannels.

Similar to round tube heat exchanger model, a sectional simulation is investigated instead of a complete configuration due to computational limitations. By applying symmetry boundary conditions at the sectional cuts, single port geometry is created in this numerical method. In addition, no meshing is applied in the inner space

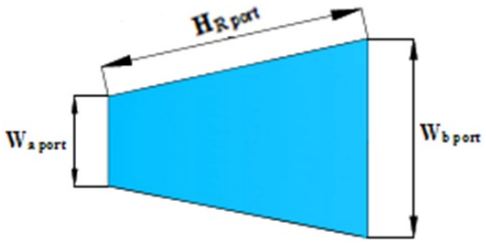

Fig. 4: Trapezoidal port geometries in round microchannel tube.

of this round microchannel tube because adiabatic assumption is exerted in this region. Furthermore, trapezoidal port shape is selected to increase the port capability on a round microchannel tube's circular configuration. In Fig. 4 trapezoidal port shape and related geometric properties are shown.

In Figs. 5, 6 a cross-sectional view of this multi-port round microchannel configuration and single port sectional view of this model are shown, respectively. In Fig. 6, Z-direction and X-Y plane represent flow direction of water and cross sectional plane, respectively.

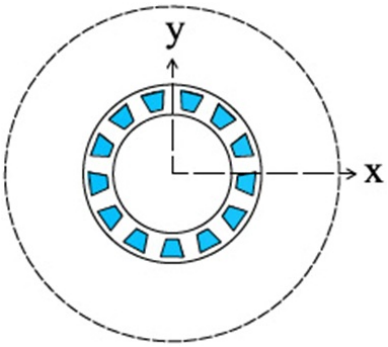

Fig. 5: Cross section of round microchannel heat exchanger.

Based on Padhmanabhan *et al.*'s (2008) study, geometric properties of round microchannel tube in tube simulation are presented in table 2.

Additionally, in order to prevent reverse flow warning and to obtain continous flow profile in this simulation, equally spaced grid points are applied for this heat exchanger model. Resultant mesh quality for this grid study is presented in Fig. 7. Moreover, this grid system is adopted after a grid-independence examination.

Table 2: Geometric specifications for round microchannel heat exchanger.

Parameter	Length (mm)
$W_{a,port}$	0.46
$W_{b,port}$	0.56
$H_{R,port}$	0.82
$H_{R,tube}$	1.3
$H_{R,jacket}$	9.86
L_{tube}	1200

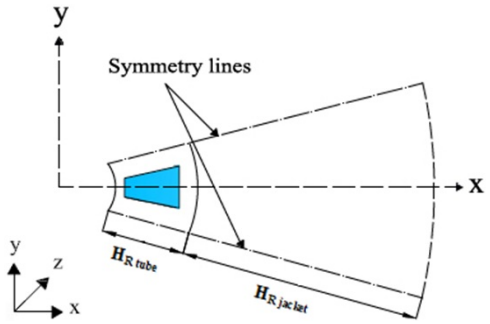

Fig. 6: Single port sectional view of round microchannel heat exchanger model.

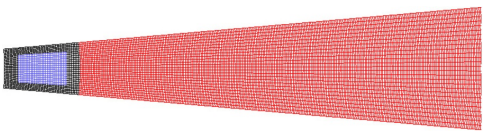

Fig. 7: Partial geometry and grid generated of round microchannel heat exchanger.

4.3. Boundary Conditions:

First, "SYMMETRY" boundary conditions are used for each sectional face cuts to provide complete solutions in these partial geometries. Furthermore, "MASS FLOW INLET" is applied to define inlet boundaries in channel flow due to available experimental data. On the other side, in order to obtain a better convergence and avoid backflows during convergence of this numerical method, "PRESSURE OUTLET" is used to define outlet boundaries in tube outlets.

In these simulations, each wall at interfaced sections separates into two faces with generating wall "Shadow". This operation makes it possible to analyze each faces of interfaced walls individually. In this investigation, a suitable boundary condition is required to define fluid/solid interface to get a conjugated solution for convection and conduction in round tube and round microchannel heat exchanger models. Hence, in wall thermal boundary condition, "Couple" option is selected to solve energy equation for the wall and its shadow simultaneously.

Finally, after creating the geometries based on indicated geometric dimensions and choosing the mesh quality and assigning appropriate boundary conditions, pre-processing in this numerical method is completed.

5. Numerical Solution:

5.1. Round Tube Heat Exchanger Computational Solution:

In order to have comparison between round tube and round microchannel heat exchanger models, it is necessary to represent round tube working condition accurately in this numerical method. As it is shown in Eq. (2), the round tube mass flow rate ($\dot{m}_{round-tube}$) is calculated by dividing the given fin and tube refrigerant mass flow rate ($\dot{m}_{fin-tube}$) into its total circuit number ($N_{circuit}$).

$$\dot{m}_{round-tube} = \frac{\dot{m}_{fin-tube}}{N_{circuit}} \tag{2}$$

Based on Johnson Control Inc's data for round tube heat exchangers, in Eq. (2), $\dot{m}_{fin-tube}$ and $N_{circuit}$ is calculated 0.12 (kg/s) and 6, respectively. For the outer water jacket, the mass flow rate is selected according to critical Reynolds number for laminar region constrains for cylindrical tubes and in order to have an identical conditions in jacket region, it is kept constant for round tube and round microchannel heat

exchanger models. In addition, initial temperature of round tube and outer water jacket in this model are defined based on Padhmanabhan *et al.*'s (2008) experimental study.

Additionally, in "Pressure outlet" flow exit condition an average pressure loss is necessary to define as gauge pressure between inlet and outlet. Therefore, Darcy-Weisbach correlation, Eq. (3), as given in Incropera *et al.* (1996) is used to estimate pressure drop and also friction factor *(f)* is appraised according to Eq. (4) in laminar flow. Resultant initial conditions for round tube heat exchanger model are listed below in table 3.

$$\Delta p = f.\frac{L}{D_h}.\frac{\rho V^2}{2} \tag{3}$$

$$f = \frac{64}{\mathrm{Re}} \tag{4}$$

Table 3: Initial conditions of round tube heat exchanger.

Parameter	Tube	Jacket
T_{in} (K)	274.7	323
V (m/s)	0.27	0.03
$\dot{m}$ (Kg/s)	0.02	0.02
Re	1584.6	1095.7
f	0.040	0.058
P_{gauge} (Pa)	180.8	1.57

In order to investigate the sudden temperature change effect on fluid thermal properties in tube and jacket of both kind of heat exchangers, fluid properties are defined as a polynomial function of temperature. Once all the initial and boundary conditions are set, iterative study is started. In order to increase the accuracy of the results, second order upwind discretization is applied in this numerical simulation for both kind of heat exchanger models.

5.2. Round Microchannel Heat Exchanger Computational Solution:

Similar to round tube heat exchanger that it was explained in previous section, initial conditions for round microchannel counter flow heat exchanger are evaluated based on Padhmanabhan *et al.*'s (2008) Experimental study. In this study, based on Johnson control Inc's data for round microchannel heat exchanger unit ($\dot{m}_{RMC,ref}$), single port mass flow rate ($\dot{m}_{port}$) which is shown in Eq. (5), is evaluated as:

$$\dot{m}_{port} = \frac{\dot{m}_{RMC,ref}}{N_{tube}.N_{RMC,port}} \tag{5}$$

In order to have a reasonable comparison between those two kind of heat exchangers, previously determined inlet conditions in round tube heat exchanger model are applied for outer water jacket in the present model. In addition, similar to previously defined round tube model, pressure drop and friction factor for round microchannel counter flow heat exchanger model are evaluated according to Eqs. (3), (4), respectively. Resultant initial conditions for this simulation are tabulated in table 4.

In the following section, numerical results for round tube and round microchannel heat exchanger models will be analyzed and a comparison between those indicated models will be performed precisely.

RESULTS AND DISCUSSION

The aim of this study is to compare the cooling effect of round tube and round microchannel tubes inside a counter flow water jacket. After the grid dependency study, computationally efficient and grid independent meshing is selected to investigate the heat transfer properties from the jacket side for both kind of heat exchangers. Furthermore, by using Eqs. (6), (7), (8), non-dimensional length, temperature and heat flux is created. By doing so, results for each heat transfer properties is simplified and in order to have a comparable results, measured units is eliminated in this solution.

Table 4: Initial conditions of round microchannel heat exchanger.

Parameter	Tube	Jacket
T_{in} (K)	274.7	323
V (m/s)	0.09	0.03
$\dot{m}(kg/s)$	3.8E-05	0.02
Re	34.3	1095.7
f	1.87	0.06
P_{gauge} (Pa)	14427.6	1.63

Non-dimensional length:

$$\eta = \frac{z}{L_{tube}} \tag{6}$$

Non-dimensional temperature:

$$\theta(\eta) = \frac{T(z) - T_{min}}{T_{max} - T_{min}} \tag{7}$$

Non-dimensional heat flux:

$$q''^{*}(\eta) = \frac{q''(z)}{q''_{max}} \tag{8}$$

6.1. Dimensionless Local Temperature:

In this section, based on Eq. (7), non-dimensional local temperature variation is obtained for round tube and round microchannel heat exchangers. According to Figs. 8, 9 temperature difference between water jacket $(\theta(\eta)_{jacket})$ and channel surface $(\theta(\eta)_{wall})$ variation is obtained for round tube and round microchannel counter flow type heat exchangers, respectively.

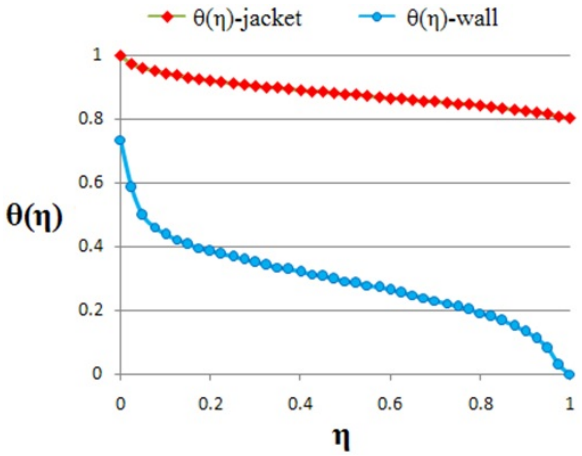

Fig. 8: Dimensionless local water jacket and wall temperature variation of round tube heat exchanger.

According to Fig. 8 in round tube heat exchanger, linear profile is observed at the tube mid section and besides at inlet and outlet sections sudden changes are reported due to constant initial temperature boundaries. Moreover, in Fig. 8, $\theta(\eta)_{wall}$ profile varies between round tube and jacket inlet temperatures. Furthermore, as it is shown in Fig. 9, an increasing temperature difference variation is observed between jacket flow and inner round microchannel tube wall and also it is obtained that the maximum difference between these value is occurred at the jacket flow exit. Furthermore, it should be indicated that because of the adiabatic internal tube surface in round microchannel heat exchanger model, $\theta(\eta)_{wall}$ couldn't reach to $\theta(\eta)_{jacket}$ value along the tube length in Z direction.

Finally, according to Figs. 8,9 , it is concluded that because of the lower refrigerant volume to surface area ratio in round microchannel heat exchanger model, faster wall temperature increase can be observed in comparison with round tube heat exchanger model.

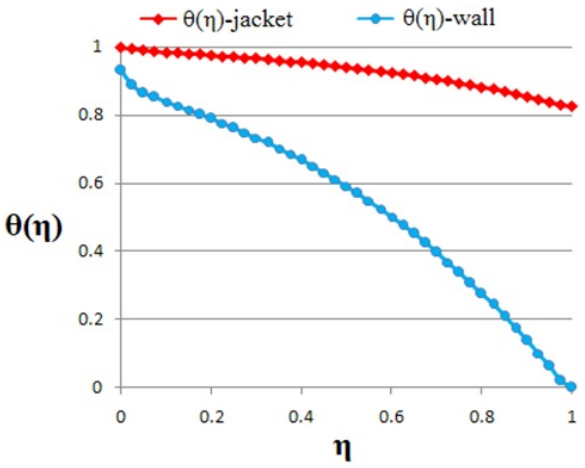

Fig. 9: Dimensionless local water jacket and wall temperature of round microchannel heat exchanger.

6.2. Dimensionless Local Heat Flux:

According to Eq. (8), non-dimensional local heat transfer rates from water jacket to channel surface ($q''^{*}(\eta)$) are calculated for round tube and round microchannel heat exchangers and local ($q''^{*}(\eta)$) variation along the tube length for both kind of heat exchanger models is presented in Fig. 10.

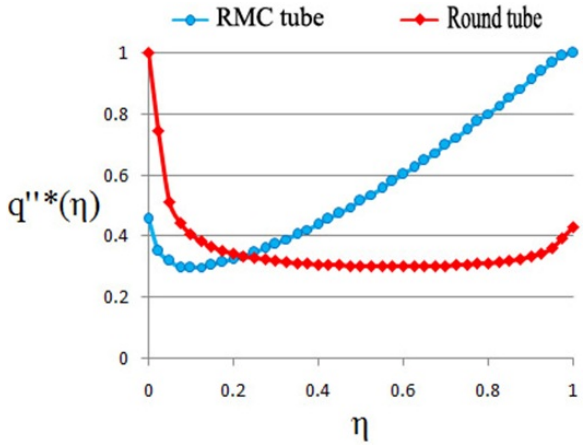

Fig. 10: Dimensionless local heat flux distribution for round tube and RMC tube heat exchanger models.

According to Fig. 10 in round tube heat exchanger model, highest heat flux value is observed at inlet section of water jacket due to sudden decrease in the fluid temperature. Then, in the mid section of this model heat transfer rate is become stable and finally, extra increase in heat flux distribution is observed at jacket outlet because of sudden decrease in wall temperature.

In Fig. 10, based on temperature profiles in Fig. 9, first a sudden decrease in $q''^{*}(\eta)$ is observed at the water jacket inlet section due to rapid change in $\theta(\eta)_{wall}$ value. Then, $q''^{*}(\eta)$ started to increase almost linearly and reached its highest value at the channel inlet where the maximum temperature difference value was obtained between jacket flow and inner RMC tube wall.

6.3. Dimensionless Local Nusselt Number:

By applying heat transfer properties which were calculated in previous sections, non-dimensional local Nusselt number along the tube length for round tube and round microchannel counter flow type heat exchangers is calculated by using Eq. (9), as:

$$Nu^{*}(\eta)=\frac{Nu(z)}{Nu_{max}} \tag{9}$$

In order to evaluate $Nu^*(\eta)$ local Nusselt number at each Z-location should be calculated based on Eq. (10) for both kind of heat exchanger models, as:

$$Nu(z) = \left(\frac{q''(z)}{T_s(z) - T_f(z)} \right) \frac{D_h}{k_f} \tag{10}$$

Consequently, by applying Eqs. (9), (10), distribution of dimensionless local Nusselt number along the tube length for round tube and round microchannel counter flow heat exchanger models are shown in Fig. 11.

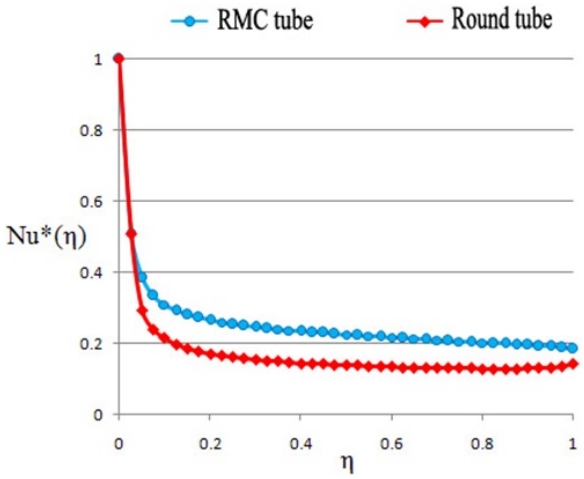

Fig. 11: Dimensionless local Nusselt number distribution for round tube and RMC tube heat exchanger models.

According to Fig. 11, it is concluded that maximum dimensionless local Nusselt number value is obtained at the water jacket inlet section due to beginning of thermal boundary layer formation which is observed in round tube and round microchannel counter flow type heat exchanger simulations. Furthermore, unlike round tube model simulation results, an almost continous decrease along the tube length in Z direction is occurred in round microchannel heat exchanger model due to similar degree of change in both temperature and heat flux distribution.

6.4. Computational Average Nusselt Number:

In order to evaluate average Nusselt number value of the jacket in round tube and round microchannel heat exchanger models, discrete local Nusselt number values along the tube length is integrated numerically. The trapezoidal rule which is shown in Eq. (11) is applied by using previously calculated Nusselt number values, as:

$$Nu_{avg-numerical} = \frac{1}{L} \int_{z_0}^{z_n - L} Nu(z)dz = \frac{\Delta z}{L} \left[\frac{Nu(z_0) + Nu(z_n)}{2} + \sum_{k=1}^{n-1} Nu(z_k) \right] \tag{11}$$

Where ΔZ is the equally spaced grid point distance and n represents the total number of grid points along the tube length in those two indicated models. Finally, numerical averaged Nusselt number of the jacket in round tube and round microchannel counterflow heat exchangers is calculated which are shown below:

Table 5: Numerical averaged Nusselt number for round tube and round microchannel heat exchanger models.

Round tube heat exchanger	9.86
RMC tube heat exchanger	12.46

6.5. Validation Results for Round Tube Heat Exchanger Model:

Based on Eq. (12), validation of this Numerical method is performed for round tube heat exchanger model and computational results are compared with corresponding Driker and Meyer's analytical Nusselt number correlation for concentric annuli (Dirker, 2005) as:

$$\mathrm{Nu}_{\text{avg-analytical}} = C_0 \,\mathrm{Re}_{D_h}^{C_1} \,\mathrm{Pr}_f^{\frac{1}{3}} \left(\frac{\mu_f}{\mu_{wall}} \right)^{0.14} \tag{12}$$

Where,

$$C_0 = \frac{0.003a^{1.86}}{0.063a^3 - 0.674a^2 + 2.225a - 1.157} \tag{13}$$

$$C_1 = 1.013e^{-0.067a} \tag{14}$$

$$\mathrm{Re}_{D_h} = \frac{\rho_f V D_h}{\mu_f} \tag{15}$$

$$D_h = (D_{jacket} - D_{round-tube-out}) \tag{16}$$

and,

$$a = \frac{D_{jacket}}{D_{round-tube-out}} \tag{17}$$

By calculating fluid properties (ρ_f, μ_f, Pr_f and μ_{wall}) in this numerical method, corresponding fluid properties are computed and then by substituting these variables in Eq. (12), annular jacket side Nusselt number for round tube heat exchanger model is calculated as:

$$Nu_{avg-analytical} = 8.89$$

Finally, in this heat exchanger model, the difference between computationally obtained Nusselt number ($Nu_{avg\text{-}Numerical}$) and its corresponding analytical correlation ($\mathrm{Nu}_{avg\text{-}analytical}$) is reported as 10%. It is concluded that a comparison between analytical and numerical studies is provided a good agreement in refrigerant side thermal analysis of round tube counter flow heat exchanger model.

Conclusions:

In this article, three dimensional simulations of the single-phase laminar flow and forced convective heat transfer of water in round tube and round microchannel heat exchangers were investigated numerically. These numerical simulations were explained similarities and differences of heat transfer properties between round tube and round microchannel heat exchanger models. In this article, at each Z-location variation of dimensionless local temperature, non-dimensional local heat flux variation and dimensionless local Nusselt number distribution along the tube length were compared between those indicated models. Furthermore, averaged computational Nusselt number was calculated for both kind of heat exchangers and then validation results was obtained for round tube heat exchanger model. Finally, it was concluded that by using lesser refrigerant in round microchannel heat exchanger in comparison with round tube heat exchanger model, higher Nusselt number was obtained in round microchannel heat exchanger. However, compared to round tube heat exchanger model higher pressure drop was occurred in round microchannel counter flow heat exchanger model.

REFERENCES

Ambatipudi, K.K., M.M. Rahman, 2000. Analysis of conjugate heat transfer in microchannel heat sinks, Numerical Heat Transfer; Part A: Applications, 37(7): 711-731.

Celata, G.P., M. Cumo, V. Marconi, S.J. McPhail, G. Zummo, 2006. Microtube liquid single-phase heat transfer in laminar flow, International Journal of Heat and Mass Transfer, 49(19-20): 3538-3546.

Dirker, J., J.P. Meyer, 2005. Convective heat transfer coefficients in concentric annuli, Heat Transfer Engineering, 26(2): 38-44.

Federov, A.G., R. Viskanta, 2000. Three-dimensional conjugate heat transfer in the microchannel heat sink for electronic packaging, International Journal of Heat and Mass Transfer, 43(3): 399-415.

Incropera, F.P., D.P. Dewitt, 1996. Fundamentals of Heat and Mass Transfer, Fourth edition, Wiley, New York.

Keogh, A., 2007. Microchannel heat exchangers, IEA Heat Pump Centre, 25(3): 15-17.

Lelea, D., S. Nishio, K. Takano, 2004. The experimental research on microtube heat transfer and fluid flow of distilled water, International Journal of Heat and Mass Transfer, 47(12-13): 2817-2830.

Mokrani, O., B. Bourouga, C. Castelain, H. Peerhossaini, 2009. Fluid flow and convective heat transfer in flat microchannels, International Journal of Heat and Mass Transfer, 52(5-6): 1337-1352.

Maranzana, G., I. Perry, D. Maillet, 2004. Mini- and micro-channels: Influence of axial conduction in the walls, International Journal of Heat and Mass Transfer, 47(17-18): 3993-4004.

Peng, X.F., G.P. Peterson, 1995. The effect of thermofluid and geometrical parameters on convection of liquids through rectangular microchannels, International Journal of Heat and Mass Transfer, 38(4): 755-758.

Padhmanabhan, S., L. Cremaschi, D. Fisher, J. Knight, 2008. Comparison of frost and defrost performance between microchannel coil and fin and tube coil for heat pump systems, International Refrigerant and Air Conditioning Conference at Purdue, July 14-17 2008: 1-8.

Qu, W.,; I. Mudawar, 2002. Analysis of three-dimensional heat transfer in microchannel heat sinks, International Journal of Heat and Mass Transfer, 45(19): 3973-3985.

Rahman, M.M., 2000. Measurements of heat transfer in microchannel heat sinks, International Communications in Heat and Mass Transfer, 27(4): 495-506.

Tuckerman, D.B., R.F.W. Pease, 1981. High-performance heat sinking for VLSI, Electron Device Letters, 2(5): 126-129.

Tuckermann, D.B., R.F. Pease, 1982. Optimized convective cooling using micromachined structure, J. Electrochem. Soc., 129(3): C98.

Wang, G., L. Hao, P. Cheng, 2009. An experimental and numerical study of forced convection in a microchannel with negligible axial heat conduction, International Journal of Heat and Mass Transfer, 52(3-4): 1070-1074.